Optimal Trajectory Tracking for a Magnetically Driven Microswimmer

Jake Buzhardt and Phanindra Tallapragada

Abstract— **Remotely actuated micro-scale swimming robots have received considerable research attention in recent years due to their promising potential for biomedical applications such as minimally invasive drug delivery. An important requirement for such applications is the ability of the robot to track a reference trajectory. In this work, a micro-robot driven by a torque induced through an applied magnetic field is considered. The spatial and rotational dynamics are formulated in terms of the body-frame torque, which is directly related to the magnetic field in the spatial frame. Controllability of the nonlinear system is then proven using the Lie algebra rank condition. Finally, an iterative linear quadratic tracking algorithm is presented and demonstrated on the system that can track arbitrary paths with both steady and time-varying velocities.**

I. INTRODUCTION

Magnetically driven microswimmers have received increased research attention in the last decade [1], [2], primarily due to the promise of many potential biomedical applications, such as cell sorting and manipulation, minimally invasive drug delivery and diagnostics, and microsurgical assistance. For many of these applications, it will be necessary for these micro-robots to accurately move in a controlled manner through complex environments.

Taking the rotating helical bundle of many bacteria as inspiration, many works have examined the motion of helically shaped or flagellar magnetic micro-robots through a fluid [3]–[6]. While several low-Reynolds number swimming systems have been considered from an optimal control perspective, most of these works focus on deriving optimal strokes or gait sequences for deformable bodies [7]–[9], typically with the assumption of direct control over body shape changes. In this work, we consider the motion of a rigid magnetic body due a torque applied through an external magnetic field. Such micro-robots have been experimentally shown to exhibit meaningful locomotion due to a uniform magnetic field with rotating direction [10]–[12]. Alaoui-Faris *et. al* [13] showed that a simple sinusoidal oscillation pattern of the magnetic field actuation does not lead to optimal locomotion of a flagellar magnetic body. Similarly, our primary aim in this work is to determine how the magnetic field should be directed over time in order to move the body along a prescribed path with a desired speed.

Developing control algorithms based on the dynamics of a magnetically rotated body is challenging, both due to the nonlinearities of the rotational dynamics and the underactuated nature of the set of control inputs. For these reasons, we take a trajectory optimization approach [14], [15] to developing control inputs to steer the system along a desired spatial trajectory.

In particular, we implement an iterative Linear Quadratic Regulator (iLQR) control scheme [16], [17]. The iLQR method is a shooting method that determines the optimal sequence of control inputs to minimize a quadratic cost function for a nonlinear system by iteratively linearizing the system about a nominal trajectory, solving for the optimal input on the linearized system, and then generating a new nominal trajectory by applying an improved input to the nonlinear system. This method has key advantages in that it can achieve fast convergence through the utilization of a Riccatti difference equation to solve the discrete-time, linear optimal control problem [17]. Also, in solving the optimal control problem in this manner, we generate not only the optimal control sequence to drive the system along a desired trajectory, but also an optimal feedback law to stabilize the system to the optimal trajectory. While this feedback law is derived using linearized dynamics, it is locally valid in a region surrounding the optimal trajectory.

The remainder of the paper is organized as follows. In Section II, we derive the model of the swimmer locomotion in terms of the governing fluid dynamics and an orientation parameterization to describe the body's rotations. In Section III, we use standard techniques from geometric nonlinear control theory to show that the system is locally controllable in terms of the two independent components of the body-frame torque. In Section IV, we describe the iterative algorithm used to optimize the trajectory of the nonlinear system. Finally, in Section V, we demonstrate this method with two numerical simulations: one on a steady, planar, circular trajectory, and another on an unsteady, three dimensional trajectory. We present results there for the optimal control sequence both in terms of the body-frame torque and the spatially-fixed magnetic field.

II. MODEL OF SWIMMER MOTION

The motion of the artificial swimmers considered in this work is described by very small length and velocity scales. In such a setting, the fluid motion generated by the particles is dominated by viscous forces, while inertial forces are considered negligible. Therefore, the fluid dynamics are well-described by the Stokes equations.

The linearity of the Stokes equations implies that the velocity $\mathbf{V}$ and angular velocity Ω of a body moving through a viscous fluid are linearly proportional to the force $\mathbf{F}$ and torque $\mathbf{T}$ acting on the body. This linear map is known as

Jake Buzhardt (jbuzhar@g.clemson.edu) and Phanindra Tallapragada (ptallap@clemson.edu) are with the Department of Mechanical Engineering, Clemson University, Clemson, SC.

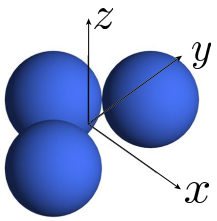

Fig. 1. Schematic of the microswimmer considered in this paper, shown in the chosen body-fixed frame of reference.

the mobility relationship and is given here by

$$\begin{pmatrix} \mathbf{V}_b \\ \Omega_b \end{pmatrix} = \begin{pmatrix} \mathbf{K} & \mathbf{C} \\ \mathbf{C}^\mathsf{T} & \mathbf{M} \end{pmatrix} \begin{pmatrix} \mathbf{F}_b \\ \mathbf{T}_b \end{pmatrix} \tag{1}$$

where the subscript b indicates that the variables are defined in a body-fixed frame of reference. Here each of the sub-matrices $\mathbf{K}$, $\mathbf{C}$, and $\mathbf{M}$ are 3×3 matrices that depend solely on the geometry of the body. Therefore, for a rigid body, as considered here, the mobility matrix is constant when defined in a body-fixed frame. While the framework given here is general enough to apply to any rigid body, a particular geometry composed of three rigidly connected magnetic spherical particles with a 90° bend is considered, as this is one of the simplest rigid geometries capable of achieving torque-driven locomotion [12], [18], [19]. This geometry is depicted in Fig. 1. The mobility relationship for this three sphere configuration has been derived previously in Refs [19]–[21]. In this work, we use the mobility matrix as derived using the Stokesian Dynamics algorithm [22]–[24], as explained in [21].

To transform these velocities from the body-fixed frame of reference to a spatially-fixed frame, we parametrize the orientation of the body using the ZXZ Euler angles so that the transformation matrix from spatial frame to body frame is given by $\mathbf{R}(\Theta) \triangleq \mathbf{R}_z(\psi)\mathbf{R}_x(\theta)\mathbf{R}_z(\phi)$ where $\mathbf{R}_x$ and $\mathbf{R}_z$ are the rotation matrices about the body-frame x and z axes by the given angles. Here we have also introduced the shorthand notation $\Theta \triangleq \begin{pmatrix}\phi & \theta & \psi\end{pmatrix}^\mathsf{T}$. Also, since these rotation matrices are orthogonal, the inverse transformation from the spatial frame to the body-fixed frame is given by $\mathbf{R}^{-1}(\Theta) = \mathbf{R}^\mathsf{T}(\Theta)$. Furthermore, the relationship between the body-frame angular velocity and the Euler angle rates of change can be defined such that $\Omega_b = \mathbf{E}(\Theta)(d\Theta/dt)$ [25].

In this work, we direct our attention toward microswimmers driven by a torque imparted on the body through an externally applied magnetic field, $\mathbf{B}$. Approximating the swimmer's magnetization as a single, permanent magnetic dipole $\mathbf{m}_b$, this torque is computed as $\mathbf{T}_b = \mathbf{m}_b \times \mathbf{R}(\Theta)\mathbf{B}$ and we assume that there are no external forces acting on the swimmer body, $\mathbf{F}_b = \mathbf{0}$.

Combining the mobility expression with the rotation kinematics, the spatial frame velocity can be related to the applied torque as

$$\frac{d\mathbf{X}}{dt} = \mathbf{R}^\mathsf{T}(\Theta)\,\mathbf{C}\,\mathbf{T}_b \tag{2}$$

where $\mathbf{X} = \begin{pmatrix} x & y & z\end{pmatrix}^\mathsf{T}$ is the vector of the spatial frame position coordinates. The Euler angle rates of change are also related to the driving torque as follows.

$$\frac{d\Theta}{dt} = \mathbf{E}^{-1}(\Theta)\,\mathbf{M}\,\mathbf{T}_b \tag{3}$$

We note here that in the following, the body-frame torque $\mathbf{T}_b$ is considered as the control input, while in a physical setting, the magnetic field $\mathbf{B}$ is directly controlled from the spatial frame. This formulation is useful, as these body frame torques can be fed forward to compute a spatial frame magnetic field input. This computation is possible, as long it is ensured that the computed torques are orthogonal to the magnetic moment vector; that is, $\mathbf{m}_b \cdot \mathbf{T}_b = 0$. To ensure this orthogonality, a component of the torque vector may be algebraically eliminated , effectively reducing the number of control inputs from three to two as

$$\mathbf{T}_b = \left(\frac{-m_y T_y - m_z T_z}{m_x}, T_y, T_z\right)^\mathsf{T} \tag{4}$$

where $(m_x \neq 0, m_y, m_z)$ are the components of the magnetic moment of the swimmer in the body frame. Substituting (4) into (2) and (3) and denoting the state vector $\xi \triangleq \begin{pmatrix}\mathbf{X}^\mathsf{T} & \Theta^\mathsf{T}\end{pmatrix}^\mathsf{T}$ one obtains the control system

$$\frac{d\xi}{dt} = g_1(\xi)u_1 + g_2(\xi)u_2 \triangleq g(\xi, u) \tag{5}$$

where $u_1 = T_y$, $u_2 = T_z$ and the vector fields g_1 and g_2 are defined by the coeffiecients of T_y and T_z respectively.

III. CONTROLLABILITY

Equation (5) defines a driftless control affine system on the manifold $\mathscr{M} = SE(3)$. In this section we show that the position of the swimmer is controllable using the control input $(u_1, u_2) = (T_y, T_z)$. We show the controllability through the application of the *Lie algebra rank condition* (LARC) [26]–[28]. For proper application of this condition, it is necessary that the drift and control vector fields associated with the system be analytic. However, in the previously defined Euler angle orientation parameterization, the transformation from $d\Theta/dt$ to Ω_b given by $\mathbf{E}$ becomes singular for some values of Θ. Therefore, the inverse transformation is not defined for all configurations, resulting in control vector fields that are not analytic on the configuration manifold. Specifically, the transformation becomes singular when the x-axis rotation angle θ becomes equal to an integer multiple of π. We therefore show controllability on $\mathscr{M} - \{\theta = n\pi\}$, $n \in \mathbb{Z}$. We note that the singularity at $\theta = n\pi$ does not represent any physical phenomenon, but rather is an artifact of this parameterization of the group $SO(3)$.

The *Lie bracket* of two vector fields g_i and g_j is defined as follows.

$$[g_1, g_2] = \nabla g_j\, g_i - \nabla g_i\, g_j \tag{6}$$

We then define the distribution Δ_ξ as the distribution generated by the vector fields g_1, g_2, and all possible Lie brackets of g_1 and g_2. The LARC is a necessary and sufficient condition for *accessibility* [27], [28], which requires that

$\dim\Delta_\xi = 6$ for the system (5). Since the system of Eq. 5 is driftless, the satisfaction of the LARC at a point ξ_0 implies that the system is controllable from ξ_0 because the Lie algebra associated with the distribution Δ_{ξ_0} then spans the tangent space $T_{\xi_0}\mathscr{M}$ [28].

Through symbolic computations in the software `Maple` we find that the distribution

$$\Delta_\xi = \text{span}\Big\{ g_1, g_2, [g1, g2], [g1, [g1, g2]], \\ [g2, [g1, g2]], [g2, [g1, [g1, g2]]] \Big\}$$

is such that $\dim\Delta_\xi = 6$ for all $\xi \in \mathscr{M} - \{\theta = n\pi\}$. This shows that from any initial configuration ξ_0, the system can be driven in any spatial coordinate direction in an arbitrarily small amount of time.

IV. TRAJECTORY TRACKING

Having established in the previous section III that the swimmer can be propelled in any direction in an arbitrarily small time, in this section we describe the iLQR tracking controller [16], [17]. The work of Sideris and Bobrow [17] serves as our main reference in implementing this algorithm and we direct readers there for a more complete treatment, but we will give a brief overview here.

We begin by discretizing the continuous time system of Eq. (5) using a simple Euler integration scheme as

$$\xi_{i+1} = \xi_i + \Delta t\, g(\xi_i, u_i) \triangleq g_d(\xi_i, u_i) \tag{7}$$

where the subscript i denotes the discretized timestep and Δt is the sampling period. Then for a given desired state trajectory ξ_i^*, $i = 1,\ldots,N$ and a given desired control trajectory u_i^*, $i = 1,\ldots N-1$, we seek the state sequence ξ_i and control sequence u_i, together satisfying the dynamics of Eq (7) and starting from a given initial state ξ_0, that minimize the following quadratic performance index.

$$J = \frac{1}{2}(\xi_N - \xi_N^*)^\intercal Q_N (\xi_N - \xi_N^*) + \frac{1}{2}(u_0 - u_0^*)^\intercal R (u_0 - u_0^*) \\ + \frac{1}{2}\sum_{i=1}^{N-1} \Big\{ (\xi_i - \xi_i^*)^\intercal Q (\xi_i - \xi_i^*) + (u_i - u_i^*)^\intercal R (u_i - u_i^*) \Big\} \tag{8}$$

In Eq. (8), Q and Q_N are symmetric, positive semi-definite weighting matrices and R is a symmetric, positive definite control weighting matrix.

Then, starting from iteration $k = 0$, we let $U_k^o = \begin{pmatrix} u_0^o & \cdots & u_{N-1}^o \end{pmatrix}$ be an arbitrary nominal control sequence. The corresponding nominal state trajectory $\Xi_k^o \triangleq \begin{pmatrix} \xi_1^o & \cdots & \xi_N^o \end{pmatrix}$ is computed by recursively computing the dynamics $\xi_{i+1}^o = g_d(\xi_i^o, u_i^o)$ from the given initial condition $\xi_0^o = \xi_0$.

We proceed by linearizing the discretized dynamics of Eq. (7) about the nominal state sequence Ξ_k^o and the nominal control sequence U_k^o. For this, we define the linear, time-varying state and control matrices as

$$A_i \triangleq \left.\frac{\partial g_d}{\partial \xi_i}\right|_{\xi_i^o,\, u_i^o} \qquad \text{and} \qquad B_i \triangleq \left.\frac{\partial g_d}{\partial u_i}\right|_{\xi_i^o,\, u_i^o}. \tag{9}$$

Further, we define the deviations from the nominal sequences as

$$\overline{\xi}_i \triangleq \xi_i - \xi_i^o \qquad \text{and} \qquad \overline{u}_i \triangleq u_i - u_i^o \tag{10}$$

and the deviation of the desired sequence from the nominal sequences as

$$\overline{\xi}_i^* \triangleq \xi_i^* - \xi_i^o \qquad \text{and} \qquad \overline{u}_i^* \triangleq u_i^* - u_i^o\,. \tag{11}$$

With this, we consider the following linear-quadratic optimal control problem on each iteration k.

$$\begin{aligned} \min_{\overline{U}_k} \ \overline{J} \quad = \quad & \frac{1}{2}(\overline{\xi}_N - \overline{\xi}_N^*)^\intercal Q_N (\overline{\xi}_N - \overline{\xi}_N^*) \\ & + \frac{1}{2}(\overline{u}_0 - \overline{u}_0^*)^\intercal R (\overline{u}_0 - \overline{u}_0^*) \\ & + \frac{1}{2}\sum_{i=1}^{N-1} \Big\{ (\overline{\xi}_i - \overline{\xi}_i^*)^\intercal Q (\overline{\xi}_i - \overline{\xi}_i^*) \\ & \qquad + (\overline{u}_i - \overline{u}_i^*)^\intercal R (\overline{u}_i - \overline{u}_i^*) \Big\} \\ \text{subject to:} \quad & \overline{\xi}_{i+1} = A_i \overline{\xi}_i + B_i \overline{u}_i \quad \text{for} \quad i = 0,\ldots,N-1 \\ & \overline{\xi}_0 = 0 \end{aligned} \tag{12}$$

In Eq. (12), $\overline{U}_k$ is the matrix containing all elements of the sequence of control deviations from nominal at stage k of the algorithm, $\overline{U}_k \triangleq \begin{pmatrix} \overline{u}_0 & \ldots & \overline{u}_{N-1} \end{pmatrix}$.

The minimization problem given by Eq. (12) is a standard time-varying, finite horizon linear-quadratic optimal tracking problem. The solution to such a problem may be found by solving a Riccati difference equation backwards in time from a final condition based on the terminal cost Q_N to obtain a optimal proportional feedback control law for the linearized system (see [17], [29]). The optimal control sequence and corresponding optimal state trajectory are then found by recursively applying the linearized dynamics

$$\overline{\xi}_{i+1} = A_i \overline{\xi}_i + B_i \overline{u}_i \tag{13}$$

forward in time from an initial condition $\overline{\xi}_0 = 0$.

This process yields the deviation $\overline{U}_k$ from the nominal control sequence that solves the tracking problem for nonlinear system linearized about the nominal control sequence U_k. As proven in Ref. [17], the deviation sequence $\overline{U}_k$ provides a descent direction in the search for a control sequence U that minimizes the cost function of Eq. (8) subjected to the constraint of the true nonlinear dynamics of Eq. (7). Therefore, the improved control input sequence is given by

$$U_k = U_k^o + \alpha_k \overline{U}_k \tag{14}$$

where $\alpha_k \in (0, 1]$ is an appropriate stepsize. The corresponding state trajectory Ξ_k can then be computed by recursively solving the nonlinear dynamics of Eq. (7) forward in time from the given initial condition ξ_0 by applying the control sequence U_k.

Finally, the algorithm proceeds by setting this improved trajectory to be the nominal trajectory at the next stage of the algorithm and incrementing the stage count k.

$$X_{k+1}^o = X_k \quad , \quad U_{k+1}^o = U_k \quad , \quad k = k+1$$

The algorithm then continues on the next stage by re-linearizing the nonlinear dynamics about the new nominal trajectory and then re-solving a new linear-quadratic optimal tracking problem. A more complete description of the algorithm, along with proofs and conditions on convergence, is given by Sideris and Bobrow [17].

V. NUMERICAL RESULTS

In this section, we present results of numerical simulations, conducted in MATLAB in which the iterative LQR algorithm described in Section IV is applied to a trajectory tracking problem for a three-sphere microswimmer. As previously detailed, this swimmer is driven by a body-frame torque induced through a magnetic field controlled from the spatial frame.

For these simulations we assume a permanent magnetic moment vector $\mathbf{m}_b = \|\mathbf{m}_b\|\hat{\mathbf{m}}_b$ where the magnitude is set to $\|\mathbf{m}_b\| = 4.0 \times 10^{-15}$ J/T, based on the values reported by Cheang *et. al* [12]. The direction $\hat{\mathbf{m}}_b$ is parameterized by the spherical coordinate angles A and Φ such that

$$\hat{\mathbf{m}}_b = \begin{pmatrix} \sin\Phi\sin A & \cos\Phi & \sin\Phi\cos A \end{pmatrix}^\mathsf{T}. \tag{15}$$

In the simulations shown here, the angles A and Φ are chosen so that all three components of vector are nonzero. The values used are $A = \pi/8$ and $\Phi = \pi/4$ radians. Further, based on the value reported by Cheang *et. al*, we constrain the applied magnetic field to have a magnitude $\|\mathbf{B}\| = 5.0$mT. With this, the upper bound on the magnitude of the velocity v of the swimmer is $v \leq \|\mathbf{C}\| \cdot \|\mathbf{m}_b\| \cdot \|\mathbf{B}\|$ where $\mathbf{C}$ is the coupling mobility of Eq. (1).

In the application of the iterative LQR algorithm, there is a design choice to be made in choosing the weighting matrices Q, R, and Q_N. Since we are interested only in tracking a spatial position sequence without regard for the orientation of the body, we choose the matrix Q to be of the form $Q = q \cdot \mathrm{diag}[1, 1, 1, 0, 0, 0]$ where q is the magnitude of the penalty placed on each of the spatial coordinate states at each timestep in the cost function. The weighting matrix R is required to be positive definite in order to solve the Riccatti difference equation. So, R is chosen to be of the form $R = r \cdot \mathrm{diag}[1, 1]$ where r is the magnitude of the penalty placed on each of the independent control inputs T_y and T_z at each timestep.

One disadvantage of the iterative LQR algorithm as presented here is that there is no rigorous means of enforcing inequality constraints involving either the states or the inputs. In this problem, there is an upper bound on the magnitude of the torque that can be applied on the swimmer based on the magnitudes of the swimmer magnetization and the the applied magnetic field, given by $\|\mathbf{T}_b\| \leq \|\mathbf{m}_b\| \cdot \|\mathbf{B}\|$. Since this constraint cannot be rigorously enforced, we instead use it to guide our choice of the weighting parameters q and r. To choose these values, we conduct a numerical search over a range of the ratio q/r. The value of the ratio q/r is then chosen to minimize the total tracking error of the trajectory without requiring a torque magnitude that exceeds 80% of the upper bound.

The choice of the sampling time parameter Δt, as shown in Eq. (7) can also have significant impact on the quality of results produced by this algorithm. Since the discretization method employed here is a simple first-order Euler scheme, it is necessary to maintain a small sampling time so that the discretized dynamics remain a good approximation of the continuous time system. In the simulations presented herein, the sampling time is chosen to be $\Delta t = 1.6667 \times 10^{-4}$ seconds. The requirement for such a small sampling time impacts the run-time of the algorithm, but as this algorithm is not designed for an online computation in which an optimal control sequence is computed in real time over a finite horizon, a long run-time is acceptable. Instead of an online optimization scheme, a more effective choice may be to use the iterative LQR algorithm to compute the optimal control sequence offline, before using a stabilizing controller to reject disturbances and drive the system back to the optimal trajectory. A major advantage of the iterative LQR algorithm is that in its solution, it provides not only the optimal control sequence, but also an optimal feedback stabilization law for the linearized system, which is also locally valid for the nonlinear system in a region surrounding the optimal trajectory.

As mentioned previously, for a given body-frame torque, for example as generated by the iterative LQR algorithm, a body-frame magnetic field to generate this torque can be found as long as the torque vector is orthogonal to the swimmer's magnetic moment vector. Both of these conditions are met in these simulations, so the body frame magnetic field is computed as

$$\mathbf{B}_b = \frac{\mathbf{T}_b \times \mathbf{m_b}}{\mathbf{m}_b \cdot \mathbf{m}_b} + \gamma \mathbf{m}_b$$

where γ is an arbitrary scalar. Further, as long as the swimmer's orientation, Θ is known, this magnetic field may be transformed to the spatial frame as $\mathbf{B} = \mathbf{R}^\mathsf{T}(\Theta)\mathbf{B}_b$. The arbitrary constant γ is handled by using the constraint that the magnetic field magnitude be $\|\mathbf{B}\| = 5.0$ mT to algebraically eliminate this additional unknown.

In the following subsections, we present two numerical examples. In the first, we show that the swimmer is capable of tracking a constant-speed, circular trajectory using the iterative LQR algorithm. In the second, we demonstrate that the swimmer can track a helical trajectory of varying curvature and desired velocity. In both simulations, the magnitude of the spatial deviation from the desired trajectory is on the order of 0.02 μm at any instant in time. We also present and discuss the spatial frame magnetic fields required to generate this trajectory.

A. Example: Steady Circular Tracking

Starting from an initial condition

$$\xi_0 = \begin{pmatrix} 10 & 0 & 0 & \pi/10 & \pi/10 & \pi/10 \end{pmatrix}^\mathsf{T} \tag{16}$$

we consider the desired spatial frame position coordinate trajectory

$$\mathbf{X}^* = \begin{pmatrix} 10\cos(0.2t) & 10\sin(0.2t) & 0 \end{pmatrix}^\mathsf{T} \tag{17}$$

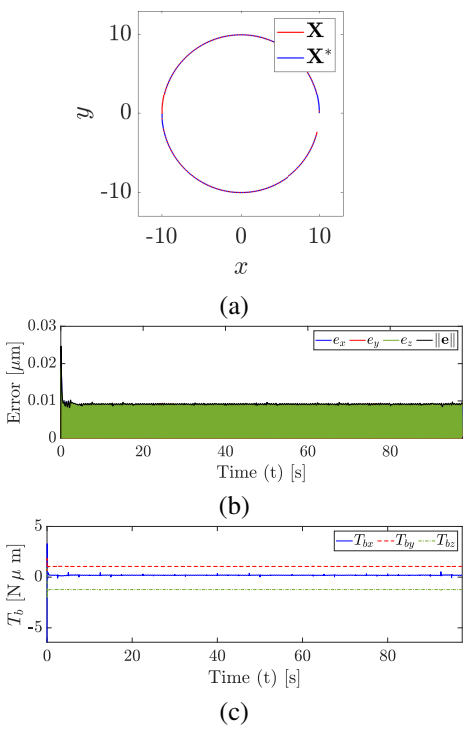

Fig. 2. Trajectory tracking results for a steady circular path in the spatial *xy*-plane. (a) Desired spatial trajectory $\mathbf{X}$ and achieved trajectory $\mathbf{X}^*$ (b) Tracking error $\mathbf{e} = |\mathbf{X} - \mathbf{X}^*|$ (c) Body frame torque $\mathbf{T}_b$ required to generate the trajectory in $\mathbf{X}$ shown in (a)

To solve the problem using the methods described above, we apply the algorithm in a receding horizon manner, in which the optimal control sequence is computed over a 5 second horizon. Then this horizon is shifted forward in time by 2.5 seconds, using the latter half of the solution for the previous horizon as the initial nominal trajectory in the next call of the algorithm. This sort of iteration is applied to construct the optimal control sequence to track the desired trajectory for a timespan of approximately 100 seconds. The results of this simulation are depicted in Fig. 2 (a), with the corresponding spatial frame magnetic field inputs shown in Fig. 3.

These results indicate that in order to achieve optimal tracking of a circular trajectory with constant speed, values of the body frame torques are found so that they can remain nearly constant to achieve the tracking, as is apparent in Fig. 2 (c). Since these torques then cause the swimmer to rotate relative to the spatial frame of reference, the magnetic field necessary to generate these torques is periodically rotating, with its axis of rotation changing direction, remaining nearly parallel to the *xy*-plane as indicated in Fig. 3.

B. Example: Unsteady Serpentine Tracking

Starting from an initial condition

$$\xi_0 = \begin{pmatrix} 0 & 0 & 0 & 0 & \pi/10 & \pi/10 \end{pmatrix}^\mathsf{T} \tag{18}$$

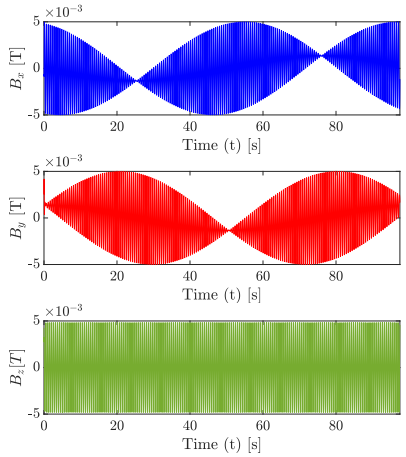

Fig. 3. Individual components of the spatial frame magnetic field $\mathbf{B}$ needed to produce the trajectory shown in Fig. 2 (a). Note that the magnetic field is constrained to a magnitude $\|\mathbf{B}\| = 5.0$ mT

we consider the desired spatial frame position trajectory given by

$$\mathbf{X}^* = \begin{pmatrix} 5\sin(0.07t) & 15(1-\cos(0.03t)) & 0.1t \end{pmatrix}^\mathsf{T} \tag{19}$$

The resulting trajectory from the implementation of the tracking algorithm as described above is given in Fig. 4, along with the necessary body frame torque sequence required to generate this trajectory. The spatial frame magnetic field required to generate this optimal trajectory is given in Fig. 5. These results indicate that the torques required to generate the trajectory no longer remain constant, as the desired velocity and curvature change in time. The magnetic field required to generate this body-frame torque is given in Fig. 5. It can be seen that in regions of the path where high swimmer velocities are required, the magnetic field is forced to oscillate with a higher frequency. Further, as the desired direction changes, the direction of the axis of rotation of the field changes to direct itself along the desired path.

VI. CONCLUSION

The nonlinear optimal trajectory tracking problem has been investigated for a magnetically-actuated, torque-driven microswimmer composed of three magnetic spheres arranged rigidly with a 90° bend. Through techniques from geometric control theory, it has been shown that the system is locally controllable using the two independent components of the body frame torque as input. Further, it was shown that these torques are directly relatable to the spatial frame magnetic field input. With this, an algorithm was presented for computing a sequence of inputs to optimally drive the system along a desired trajectory. The procedure relies on the linearization of the nonlinear dynamics about a sequentially improving nominal trajectory. Thus this algorithm also returns a feedback structure that can be used to stabilize the system to the optimal trajectory. Finally, the efficacy of the algorithm was demonstrated through numerical simulation of two examples, showing that the method can provide accurate

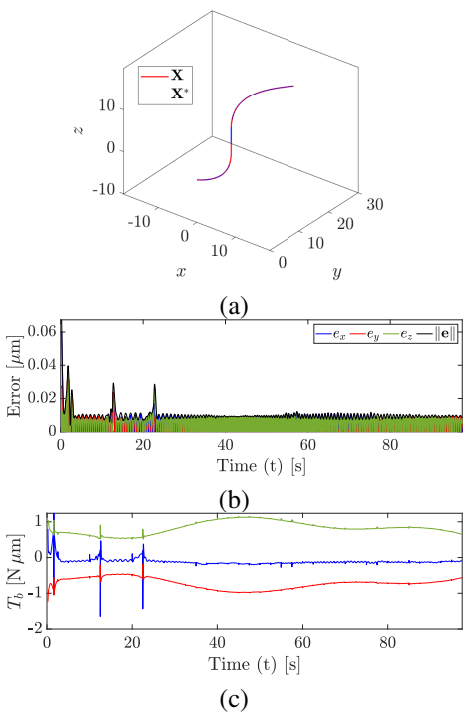

Fig. 4. Trajectory tracking results for an unsteady serpentine path in the spatial position coordinates . (a) Desired spatial trajectory $\mathbf{X}$ and achieved trajectory $\mathbf{X}^*$ (b) Tracking error $\mathbf{e} = |\mathbf{X} - \mathbf{X}^*|$ (c) Body frame torque $\mathbf{T}_b$ required to generate the trajectory in $\mathbf{X}$ shown in (a)

solutions for constant and non-constant curvature and for both steady and unsteady desired velocities.

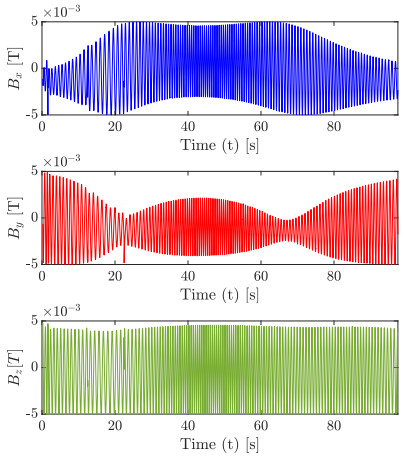

Fig. 5. Individual components of the spatial frame magnetic field $\mathbf{B}$ needed to produce the trajectory shown in Fig. 4. Note that the magnetic field is constrained to a magnitude $\|\mathbf{B}\| = 5.0$ mT

REFERENCES

[1] B. J. Nelson, I. K. Kaliakatsos, and J. J. Abbott. Microrobots for minimally invasive medicine. *Annu. Rev. Biomed. Eng.*, 12:55–85, 2010.

[2] M. Sitti, H. Ceylan, W. Hu, J. Giltinan, M. Turan, S. Yim, and E. Diller. Biomedical applications of untethered mobile milli/microrobots. *Proceedings of the IEEE*, 103(2):205–224, Feb 2015.

[3] L. Zhang, J. J. Abbott, L. Dong, B. E. Kratochvil, D. Bell, and B. J. Nelson. Artificial bacterial flagella: Fabrication and magnetic control. *Appl. Phys. Lett.*, 94:064107, 2009.

[4] A. Ghosh and P. Fischer. Controlled propulsion of artificial magnetic nanostructured propellers. *Nano Lett.*, 9(6):2243–2245, 2009.

[5] K. E. Peyer, L. Zhang, and B. J. Nelson. Bio-inspired magnetic swimming microrobots for biomedical applications. *Nanoscale*, 4(5):1259–1272, 2013.

[6] F. Alouges, A. DeSimone, L. Giraldi, and M. Zoppello. Can magnetic multilayers propel artificial microswimmers mimicking sperm cells? *Soft Robotics*, 2(3):117128, Sep 2015.

[7] S. Michelin and E. Lauga. Efficiency optimization and symmetry-breaking in a model of ciliary locomotion. *Physics of Fluids*, 22(11):111901, 2010.

[8] J. Lohéac, J. Scheid, and M. Tucsnak. Controllability and time optimal control for low reynolds number swimmers. *Acta Appl Math*, 123:175–200, 2013.

[9] R. Marchello, M. Morandotti, H. Shum, and M. Zoppello. The *n*-link swimmer in three dimensions: controllability and optimality results, 2019.

[10] A. Ghosh, D. Paria, H. J. Singh, P. L. Venugopalan, and A. Ghosh. Dynamical configurations and bistability of helical nanostructures under external torque. *Phys. Rev. E*, 86:031401, Sep 2012.

[11] L. Zhang, T. Petit, Y. Lu, B. E. Kratochvil, K. E. Peyer, R. Pei, J. Lou, and B. J. Nelson. Controlled propulsion and cargo transport of rotating nickel nanowires near a patterned solid surface. *ACS Nano*, 4(10):6228–6234, 2010.

[12] U. K. Cheang, F. Meshkati, D. Kim, M. J. Kim, and H. C. Fu. Minimal geometric requirements for micropropulsion via magnetic rotation. *Phys. Rev. E*, 2014.

[13] Y. El Alaoui-Faris, J. Pomet, S. Régnier, and L. Giraldi. Optimal actuation of flagellar magnetic micro-swimmers, 2019.

[14] J. T Betts. *Practical methods for optimal control and estimation using nonlinear programming*, volume 19. Siam, 2010.

[15] M. Kelly. An introduction to trajectory optimization: How to do your own direct collocation. *SIAM Review*, 59(4):849–904, 2017.

[16] W. Li and E. Todorov. Iterative linear quadratic regulator design for nonlinear biological movement systems. In *Proceedings of the First International Conference on Informatics in Control, Automation and Robotics - Volume 1: ICINCO*, pages 222–229. INSTICC, SciTePress, 2004.

[17] A. Sideris and J. E Bobrow. An efficient sequential linear quadratic algorithm for solving nonlinear optimal control problems. In *Proceedings of the 2005, American Control Conference, 2005.*, pages 2275–2280. IEEE, 2005.

[18] J. Happel and H. Brenner. *Low Reynolds number hydrodynamics: with special applications to particulate media*. Springer, 1983.

[19] F. Meshkati and H. Fu. Modeling rigid magnetically rotated microswimmers: Rotation axes, bistability, and controllability. *Phys. Rev. E*, 90(6):063006, 2014.

[20] K. I. Morozov, Y. Mirzae, O. Kenneth, and A. M. Leshansky. Dynamics of arbitrary shaped propellers driven by a rotating magnetic field. *Phys. Rev. Fluids*, 2017.

[21] J. Buzhardt and P. Tallapragada. Dynamics of groups of magnetically driven artificial microswimmers. *Phys. Rev. E*, 100:033106, Sep 2019.

[22] L. Durlofsky, J. F. Brady, and G. Bossis. Dynamic simulation of hydrodynamically interacting particles. *J. Fluid Mech.*, 180:2149, 1987.

[23] J. F. Brady and G. Bossis. Stokesian dynamics. *Annual Review of Fluid Mechanics*, 20:111–157, 1988.

[24] J. W. Swan, J. F. Brady, R. S. Moore, and ChE 174. Modeling hydrodynamic self-propulsion with stokesian dynamics. or teaching stokesian dynamics to swim. *Phys. Fluids*, 23(7):071901, 2011.

[25] H. Goldstein. *Classical Mechanics*. Addison-Wesley, 1980.

[26] R. Murray, Z. Li, and S. S. Sastry. *A Mathematical Introduction to Robotic Manipulation*. CRC Press, 1994.

[27] F. Bullo and A. D. Lewis. *Geometric Control of Mechanical Systems*. Springer Verlag-Berlin, 2004.

[28] A. M. Bloch. *Nonholonomic Mechanics and Control*. Springer Verlag, 2003.

[29] A.E. Bryson and Y. Ho. *Applied Optimal Control*. Routledge, 1975.